

N70 31995

**NASA TECHNICAL  
MEMORANDUM**

NASA TM X-52843

NASA TM X-52843

CASE FILE  
COPY

**TIME HISTORY PLOTS AND COMPUTER MADE  
MOVIES OF ION-POLAR MOLECULE COLLISIONS  
OF INTEREST IN MASS SPECTROMETRY**

by John V. Dugan, Jr.  
Lewis Research Center  
Cleveland, Ohio

and John L. Magee  
University of Notre Dame  
Notre Dame, Indiana

TECHNICAL PAPER proposed for presentation at  
American Society of Mass Spectrometry  
San Francisco, California, June 16-21, 1970

TIME HISTORY PLOTS AND COMPUTER MADE MOVIES OF ION-POLAR MOLECULE  
COLLISIONS OF INTEREST IN MASS SPECTROMETRY

by John V. Dugan, Jr.  
National Aeronautics and Space Administration  
Lewis Research Center  
Cleveland, Ohio

and

John L. Magee  
University of Notre Dame  
Notre Dame, Indiana

ABSTRACT

E-5772

Capture cross sections are calculated for ion-polar molecule collisions of interest in mass spectrometry. These cross section predictions are in relatively good agreement with experimental data on reaction cross sections. The collision trajectories have been studied using computer-plotter techniques. The interaction potential consists of a hard-sphere term plus the attractive polarization and ion-dipole terms. Multiple reflections corresponding to formation of long-lived complexes occur off the hard-core barrier at small ion-molecule separations. Multiple-reflection times are 10 to 500 times corresponding values for single reflections. Hindered rotation of the polar targets (suggested by time history plots) is studied by computer-made movies. This technique also offers a convenient visual means for observing the relative motion of the ion-molecule pair.

INTRODUCTION

Capture cross sections have been calculated for ion-polar molecule collisions; the interaction potential consists of classical ion-dipole plus ion-induced dipole (polarizability) terms. These capture cross sections set a rough upper limit to the reaction cross section. The ion-dipole energy transfer and formation of ion-molecule collision complexes have been studied using computer-plotter techniques. Mutual orbiting of the ion-molecule pair and hindered rotation of the dipole have also been studied via computer-made motion pictures. The latter is of particular interest for ion-molecule reactions since preferred dipole orientation favors certain reactions. This paper reports on results obtained for ion-molecule systems of particular interest in mass spectrometry.

COLLISION TARGETS

The polar targets studied were chosen mainly because they have been studied in the mass spectrometer. Their molecular constants also cover an interesting range of collision parameters. Ion-molecule reactions involving  $\text{CH}_3\text{CN}$  have been studied by Moran and Hamill.<sup>1</sup> The good

agreement between theory and mass spectrometer experimental values have been reported.<sup>2</sup> Large cross sections  $\sim 650 \text{ \AA}^2$  for  $\text{CH}_3\text{OH}$  targets were reported in refs. 3 and 4 for low ion energies. Negative ion-molecule cross sections reported for  $\text{H}_2\text{O}$  targets are roughly  $10^{-13} \text{ cm}^2$ .<sup>5</sup>

The dipole moments, polarizabilities and moments of inertia assigned to the three targets are given in Table I.  $\text{CH}_3\text{CN}$  is a symmetric top whereas  $\text{CH}_3\text{OH}$  and  $\text{H}_2\text{O}$  were approximated as symmetric tops. The two moments of inertia assigned for each target were the largest moment and the moment about the symmetry axis. This approximation should not be critical for  $\text{CH}_3\text{OH}$ ; however, for  $\text{H}_2\text{O}$  the neglected moment is approximately equal to the principal moment.<sup>6</sup> Previous comparison of capture cross sections for linear molecules and symmetric tops suggest that the cross section is independent of target geometry.<sup>7</sup>

#### ION MOLECULE INTERACTION

The ion-molecule interaction consists of the ion-permanent dipole and ion-induced dipole (polarizability) terms. The first term  $= -\mu e \cos \gamma$  where  $\mu$  is the permanent dipole moment,  $e$  is the electronic charge,  $\gamma$  is the ion-dipole orientation angle and  $r$  is the ion-molecule separation. The Langevin polarizability term is  $-\alpha e^2/2r^4$  where  $\alpha$  is the molecular polarizability which is assumed spherically symmetric. The separate cross section contributions are the Langevin cross section

$$\sigma_L = \pi(2\alpha e^2/\epsilon)^{1/2} = \pi b_L^2 \quad (1)$$

and the ion-dipole cross section.

$$\sigma_D = \pi \mu e / \epsilon \quad (2)$$

Assuming favorable orientation of the dipole, i.e.,  $\gamma = 0$ , the cross section

$$\sigma_M = \sigma_L + \sigma_D = \pi b_M^2 \quad (3)$$

is somewhat of a maximum. In equations (1) to (3),  $\epsilon$  is the relative translational energy. The ion and molecule are reflected off a hard-core potential at  $r = r_c$ . This reflection simulates ion-molecule repulsion due to the interacting electronic clouds.

## COMPUTER APPROACH

Collision quantities such as ion velocity and dipole rotational energy are plotted using values obtained by numerical integration. The time history plots are done in the coordinate system where the polar molecule is fixed at the origin.<sup>8</sup> The differential equations of motion are integrated using the variable step-length Runge-Kutta scheme of Ref. 7. Solutions of the equations include the coordinates for movie models of the colliding partners. The initial conditions and successful steps (for variables and time derivatives) are stored in a plotting array for both computer-made time history plots and movies. After the integration is completed the plotting subroutines are called. Each plotting array contains  $N + 1$  values where  $N$  is the number of successful integration steps (typically 300 to 1000).

## MOVIE MODEL

The coordinate solutions are used to draw projections of the ion and polar molecule models in the center-of-mass system. In fig. 1, a sample movie frame shows models of the ion and dipole with a clock in the upper right hand corner.<sup>9</sup> Each frame is traced on a cathode-ray-tube and photographed using the IBM 360/67 computer with the CDC DD280 plotter. A hard sphere barrier is located at an ion-molecule separation  $r_c$  equal to the sum of the ion and molecule radii. The plotted radius of each particle in the model is varied proportionately to the particle distance above (expanded) and below (contracted) the X-Y plane. The clock measures real time and moves at different rates during a collision since a variable step-size integration routine is used.

## INITIAL CONDITIONS

The initial conditions on the dependent variables and their first time derivatives are obtained using a random number generator. Trajectories were studied for ion velocities of  $5 \times 10^4$ ,  $10^5$ , and  $2 \times 10^5$  cm sec<sup>-1</sup>. Target rotators were chosen from a heat bath at rotational temperature  $T_R = 500$  K. The estimated reflection distances for the collision complex studies were 2, 2.5, and 3.0 Å for CO, HCl, and CH<sub>3</sub>CN, respectively whereas 2 Å was used as a capture distance in all cross section calculations. It should be noted that these values are somewhat (25 percent) less than the Van der Waals radii of the neutral species.<sup>10</sup>

## RESULTS

In all numerical calculations the energy equation and behavior of trajectories with time reversal were used as checks on the accuracy of the integration routine.

### Capture Cross Sections

For each impact parameter 36 to 50 trajectories were calculated for the capture cross section; these trajectories were truncated once  $r \leq 2 \text{ \AA}$ . Unlike Langevin collisions there is no all-or-nothing answer to the question of capture in ion-permanent dipole collisions for fixed initial impact parameter. For fixed values of energy and impact parameter there is a probability that the system will arrive at an ion-molecule separation corresponding to capture. The fraction of collisions resulting in such a prescribed "minimum" separation we call the capture ratio. Such a fraction can be correlated with the ion-molecule reaction probability.

CH<sub>3</sub>CN + HCl. - Results of the capture ratio  $C_R$  versus  $b^2$  are shown in Fig. 2 for the CH<sub>3</sub>CN<sup>+</sup> + CH<sub>3</sub>CN collision at two different relative velocities. Results are shown for HCl<sup>+</sup> + HCl at two different rotational energies and two ion velocities in Figs. 3(a) and (b). The plot of the Langevin "all-or-nothing" capture ratio is a step function in both Figs. 2 and 3.

A reasonable definition of the "capture collision" cross section is

$$\sigma_c \equiv \pi \int_0^{b_0} C_R(b) d(b^2) \quad (4)$$

where  $b_0$  is the impact parameter at which  $C_R$  becomes zero. The integral is simply the area under the  $C_R$  versus  $b^2$  curve. The calculated value  $b_c^2$  is compared with  $b_L^2$  (eq. (1)),  $b_D^2$  (eq. (2)), and the sum  $b_M^2$  (eq. (3)). The cross section results are relatively insensitive to the choice of cutoff ion-molecule separation (equal to 2Å for HCl and CH<sub>3</sub>CN). Figures 2 and 3 indicate that the shape of the  $C_R$  plots is sensitive to both rotational energy and ion velocity. The very large effect of the dipole is clear from comparison with the Langevin prediction for a molecule with the polarizability of CH<sub>3</sub>CN. For HCl the effectiveness of the dipole is far less than the "adiabatic" or maximum effect.

In Fig. 4(a) the calculated cross section for CH<sub>3</sub>CN is shown as a function of energy and compared with various analytical estimates. The most obvious feature of this figure is how much larger the calculated cross section is than the Langevin cross section. The calculation also shows that the effect of the dipole is not as great at low energies as predicted on the basis of the adiabatic approximation. The capture cross section  $Q_{\max}$  as assumed by the experimentalists is the integral of  $\sigma_c$  over all ion energies. This cross section is compared with the calculated capture cross section  $Q_c$  and observed reaction cross section  $Q_R$  in Fig. 4(b).

CH<sub>3</sub>OH. - The plots of  $C_R$  versus  $b^2$  are given for the CH<sub>3</sub>OH (symmetric top approximation) + CH<sub>3</sub>OH<sup>+</sup> collision in Figs. 5(a) and (b) for ion velocities of  $5 \times 10^4$  and  $10^5$  cm sec<sup>-1</sup>. The corresponding cross section  $\sigma_c$  is plotted versus relative translational energy in Fig. 5(c). It is clear that this upper limit to the reaction cross section is somewhat less than the reported values even at thermal energy ( $\epsilon_1 = kT_t$  for  $T_t = 500$  K). The O-H bond does not lie along the symmetry axis of CH<sub>3</sub>OH (i.e., CH<sub>3</sub>OH is not quite a symmetric top). However, comparison of capture cross sections for linear molecules and symmetric tops suggests that additional degrees of rotational freedom have little effect on the capture probability.<sup>7</sup> The agreement between theory and experiment (refs. 1, 3, and 4) is not as satisfactory as for the CH<sub>3</sub>CN system but this may be due to systematic experimental error.

H<sup>+</sup> + H<sub>2</sub>O. - Stockdale et al.<sup>5</sup> report cross section values of  $5 \times 10^{-13}$  cm<sup>2</sup> (lower limit) at ion energies of  $\epsilon_1 = 0.2$  eV. The maximum cross section  $\sigma_M$  computed for H<sup>+</sup> + H<sub>2</sub>O is only  $2.5 \times 10^{-14}$  cm<sup>2</sup> (250 Å<sup>2</sup>) at  $\epsilon_1 = 0.2$  eV (corresponding to an H<sup>+</sup> velocity of  $2 \times 10^6$  cm sec<sup>-1</sup>). However, the numerically calculated cross section is only  $\pi (36 \text{ Å}^2) = 113 \text{ Å}^2$  (see Fig. 6). The ratio of experimental to calculated cross section is thus roughly a factor of 45. This discrepancy does not appear explainable on the basis of the usual experimental errors. More careful experiments are clearly required to obtain reliable absolute cross section data.

#### Collision Lifetimes and Hindered Rotation

Trajectories of the ion-molecule pair have been calculated as well as capture cross sections.<sup>8,9,11</sup> Trajectory results indicate that there is a rapid interchange of energy between translational and rotational energy. This energy transfer suggests the possibility of long-lived collision complexes. Experimental evidence points to the existence of long-lived ion-molecule collision complexes.<sup>12,13</sup> Numerical lifetimes are only  $10^{-10}$  sec. To explain the long experimental lifetimes (as long as  $10^{-7}$  sec) requires consideration of additional mechanisms including participation of internal degrees of freedom. Such long-lived complexes must, therefore, be formed by inelastic collisions.

For trajectory studies it is necessary to treat the short-range interactions in some fashion. We have used the following extreme approximation; a hard inner core, i.e., at  $r = r_c$  the potential is stepwise infinite. The inward and outward trajectories are symmetric (specular reflection) for the simple Langevin potential.

The situation is different for an ion-molecule collision involving a molecule with a dipole moment. The rotating dipole alters the potential for the outward trajectory, outer turning points can be introduced and multiple reflections occur. For parameters of interest in actual collisions as many as 2000 reflections have been observed numerically with collision times  $\tau$  as large as  $10^2$  times the single reflection period.<sup>8,9</sup>

## Results of Trajectory Calculations

Results of computer calculations of ion-molecule collisions are shown in Figs. 7 to 15. These time history plots have been made using the IBM 360/67 computer with the CDC DD280 plotter. Figures 7 and 8 show the variation of velocity and rotational energy as a function of separation. The collision shown in Fig. 7, for  $\text{HCl} + \text{NO}_2^+$ , involves a single reflection. The velocity increases as the separation decreases to the critical value where the potential energy is a minimum. The rotational energy changes drastically: there is hindered rotation at the small separations.

The trajectory of Fig. 8, for  $\text{CO} + \text{Ar}^+$ , involves multiple reflections. Variation of the outer turning point is shown in this figure in the rotational energy plot.

The simplest systems on which our computations are based are essentially triatomic (i.e., diatomic rotors and monatomic ions). The trajectories do not lie in planes as is shown in Fig. 9 obtained from calculations for  $\text{CO} + \text{Ar}^+$ . This figure shows a multiple reflection collision.

Symmetric top dipolar molecules have one more degree of freedom than rigid rotors and their collisions are more complicated. Their trajectories involve more multiple reflections than rigid rotors. Figures 10 and 11 show trajectories for collisions of  $\text{CH}_3\text{CN}$  with its parent ion (i.e., as regards ion mass). These figures indicate a more effective transfer of energy between rotational and translational degrees of freedom than for the linear molecule.

Figures 12 to 15 show variations of the polar and azimuthal angles for trajectories involving multiple reflections for  $\text{HCl} + \text{NO}_2^+$ ,  $\text{CH}_3\text{CN} + \text{CH}_3\text{CN}^+$ , and  $\text{CO} + \text{Ar}^+$ . Figure 15 shows how distant some of the outer turning points in multiple reflection trajectories can be. One turning point for  $\text{CH}_3\text{CN} + \text{CH}_3\text{CN}^+$  occurs at 22 Å separation. So-called "sticky" collisions involving alkyl halide molecules have been studied in the mass spectrometer; these collisions have large cross sections in polar systems.<sup>14</sup> These collisions should be similar to the  $\text{CH}_3\text{CN} - \text{CH}_3\text{CN}^+$  collisions.

It should be noted that multiple reflections are also to be expected for collisions involving polyatomic molecules without dipole moments since actual short range potentials probably have sufficient angular dependence in most cases to produce in varying degree the same effect as dipoles.

## Lifetime Considerations

Theories of the lifetime of complexes have been considered<sup>15,16</sup> and can be applied to these cases. These theories assume that the energy of the complex is completely randomized over certain participating degrees of freedom, and the rather complicated nature of our calculated multiply-reflected trajectories would suggest that such an assumption is reasonable for our

cases. Application of any theory requires more knowledge of the potential functions of the complexes than we have at present and the discussion presented here can be only fragmentary. The simplest "theoretical" expression for the lifetime of a complex with enough energy to decompose is<sup>17</sup>

$$\tau = \tau_0 \left[ E / (E - E_b) \right]^s \approx \tau_0 \left[ (E_b + \epsilon) / \epsilon \right]^s \quad (5)$$

where  $\tau_0$  is a time parameter made up of physical constants of the complex;  $E$  is the energy of the complex with its zero point energy taken as the zero of energy;  $E_b$  is the magnitude of the binding energy of the complex;  $s$  is a parameter determined by the number of degrees of freedom of the system. We have that  $E = E_b + \epsilon$  where  $\epsilon$  is the relative energy of colliding pair. Thus  $\tau_0$  is a constant of the same magnitude as the collision time without reflections; i.e.,  $\tau_0 \approx 10^{-12}$  s.  $E_b$  is in the range of 0.5 to several eV. For the various collisions we are considering here,  $s$  varies from 0.5 to 1.0. Since  $(E_b + \epsilon) / \epsilon$  varies from about 10 to 500, we expect that the collision time should be increased by a factor of 10 to several hundred by the reflection phenomenon.

#### Computer-Made Movies of Ion-Dipole Collisions

The computer-plotter studies have been extended to the making of motion pictures of ion-dipole single- and multiple-reflection collisions. The collision movies provide instantaneous visual correlation of the relative translational motion of the pair and the dipole rotational motion. One of the most interesting phenomena observed in the movies is the hindering of the rotational motion of the dipole. The three polar rotors CO, HCl, and CH<sub>3</sub>CN are seen to be hindered by the incident ion to varying degrees.<sup>12</sup>

Figure 16 is a superposition of movie frames of a CH<sub>3</sub>CN capture collision involving only one reflection. It provides a correlated history of ion-dipole interaction. The results are not presented at equal time intervals since a variable step-size is used. The post-reflection hindering of the CH<sub>3</sub>CN rotor at 5 to 15 Å is demonstrated in the movie. It has been suggested that preferential orientation of the negative end of the dipole toward the positive ion will favor a specific chemical reaction.<sup>13</sup>

Figure 17 was obtained in the same manner as Fig. 16 except it shows 40 frames superimposed for a multiple reflection collision. This collision sequence does not show hindered rotation but presents an interesting history of translational mutual orbiting. This mutual orbiting of the ion-molecule pair is nearly symmetric for this six reflection collision. This particular collision results in approximately 0° scattering in the center-of-mass system.



### Vibrational Effects

Numerical studies of ion-dipole collisions have been extended to calculating the effects of vibrational degrees of freedom on both multiple reflection probability and average collision lifetime  $\tau_R$ . The dipole moment of the polar molecule is assumed Gaussian about the equilibrium bond separation of the oscillator. Both time history plots of collision variables and computer-made motion pictures are used to study the interaction of the ion with the oscillating dipole. Initial results have been obtained chiefly for loose (thermal) oscillators with energies of 0.036 eV. The results indicate such oscillators actually lower the fraction of multiple reflection collisions for CO but increase it for CH<sub>3</sub>CN at impact parameters greater than 8 Å. The collision lifetimes are somewhat insensitive to the presence of the oscillator for the 300 cases studied. Stiff oscillators (50 cases studied) generally lower the  $\tau_R$  value by cooling; this result is unphysical for targets vibrating initially in the ground state.

### CONCLUDING REMARKS

Numerical calculations have been made on several different features of ion-polar-molecule collisions. Calculated cross sections are in good to satisfactory agreement with experiment for CH<sub>3</sub>CN and CH<sub>3</sub>OH targets. However, there is considerable disparity between predicted and observed values for negative ion-H<sub>2</sub>O reactions. There is a clear need for more reliable absolute cross section data; the numerical results also suggest that the rotational temperature dependence of the cross section should be investigated.

The existence of long-lived ion-molecule complexes ( $\tau \approx 10^{-11} - 10^{-10}$  sec) has been demonstrated for a rotating polar target with and without vibrational effects. A more sophisticated model incorporating additional internal degrees should predict collision complex lifetimes in better agreement with experiment ( $\sim 10^{-7}$  sec). (This conclusion is based on simple lifetime predictions.) Preliminary calculations which take thermal harmonic oscillators into account remain somewhat inconclusive with regard to lifetime effects.

Time history plots of ion-dipole orientation angle have suggested that considerable hindering of the dipole occurs. Computer-made movies have proven valuable in demonstrating hindered rotation in ion-dipole collisions via instantaneous correlation of translational and rotational motion. Superimposed movie frames provide time histories of this hindered rotation and mutual orbiting of collision partners. An ultimate objective of this work is the application to more complicated processes such as ion-molecule reactions and charge exchange. In such processes it is quite clear that relatively long-lived complexes must be involved.

## REFERENCES

1. T. F. Moran and W. H. Hamill, J. Chem. Phys. 39, 1413 (1963).
2. J. V. Dugan, Jr., and J. L. Magee, J. Chem. Phys. 47, 3103 (1967).
3. Private communication, D. P. Stevenson to W. H. Hamill.
4. L. P. Theard and W. H. Hamill, Am. Chem. Soc. J. 84, 1134 (1962).
5. J. A. D. Stockdale, R. N. Compton and P. W. Reinhardt, Phys. Rev. 184, 81 (1969).
6. G. Herzberg, Infrared and Raman Spectra of Polyatomic Molecules (D. Van Nostrand Co., Inc., New Jersey, 1945).
7. J. V. Dugan, Jr., J. H. Rice, and J. L. Magee, NASA TM X-1586 (1968).
8. J. V. Dugan, Jr., and J. H. Rice, NASA TN D-5407 (1969).
9. J. V. Dugan, Jr., J. H. Rice, and J. L. Magee, Chem. Phys. Letters, 3, 323 (1969).
10. J. O. Hirschfelder, C. F. Curtiss, and R. B. Bird, Molecule Theory of Gases and Liquids (John Wiley and Sons, Inc., New York, 1964), 2nd ed.
11. J. V. Dugan, Jr., R. B. Canright, Jr., R. W. Palmer, and J. L. Magee, NASA TM X-52662 (1969); paper presented at VI Int'l Conference Electronic and Atomic Collisions, Boston; MIT Press, July 1969, pp. 333-340.
12. D. K. Bohme, D. B. Dunkin, F. C. Fehsenfeld, and E. E. Ferguson, to be published.
13. D. K. Bohme, private communication.
14. R. F. Pottie, A. J. Lorquet, and W. H. Hamill, *ibid.*, 84, 529 (1962).
15. H. M. Rosenstock, M. B. Wallenstein, A. L. Wahrhaftig, and H. Eyring, Proc. Nat'l Acad. Sci. 38, 667 (1952).
16. R. A. Marcus and O. K. Rice, J. Phys. Chem. 55, 894 (1951); R. A. Marcus, J. Chem. Phys. 20, 359 (1952).
17. M. Burton and J. L. Magee, J. Phys. Chem. 56, 852 (1952).

TABLE I

| Polar target, molecule | Dipole <sup>a</sup> moment, D.U. | Polarizability, Å <sup>3</sup> | Principal moment of inertia, I <sub>1</sub> (gm-cm <sup>2</sup> )x10 <sup>40</sup> | Ratio of moments of inertia, I <sub>2</sub> /I <sub>1</sub> |
|------------------------|----------------------------------|--------------------------------|--|---|
| CH <sub>3</sub> CN     | 3.92                             | 3.8                            | 9.12x10 <sup>1</sup>   | 0.06  |
| CH <sub>3</sub> OH     | 1.67                             | 2.4                            | 3.58x10 <sup>1</sup>   | .15   |
| H <sub>2</sub> O       | 1.86                             | 2.5                            | 1.93   | 1.51  |

<sup>a</sup>1 Debye unit (D.U.) = 10<sup>-18</sup> esu - cm.

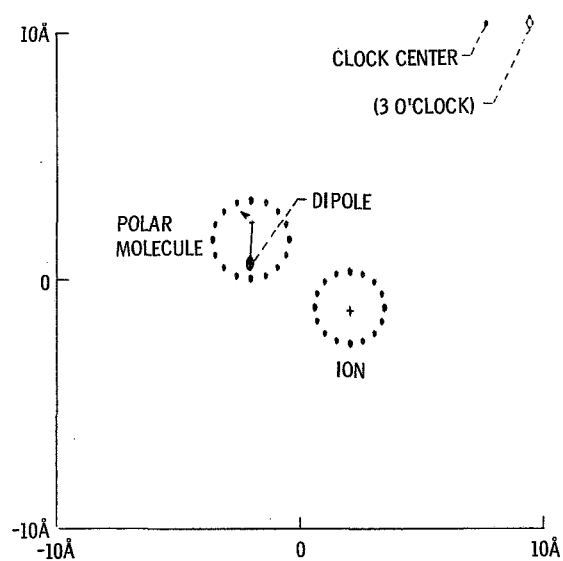


Figure 1. - Sample movie frame.

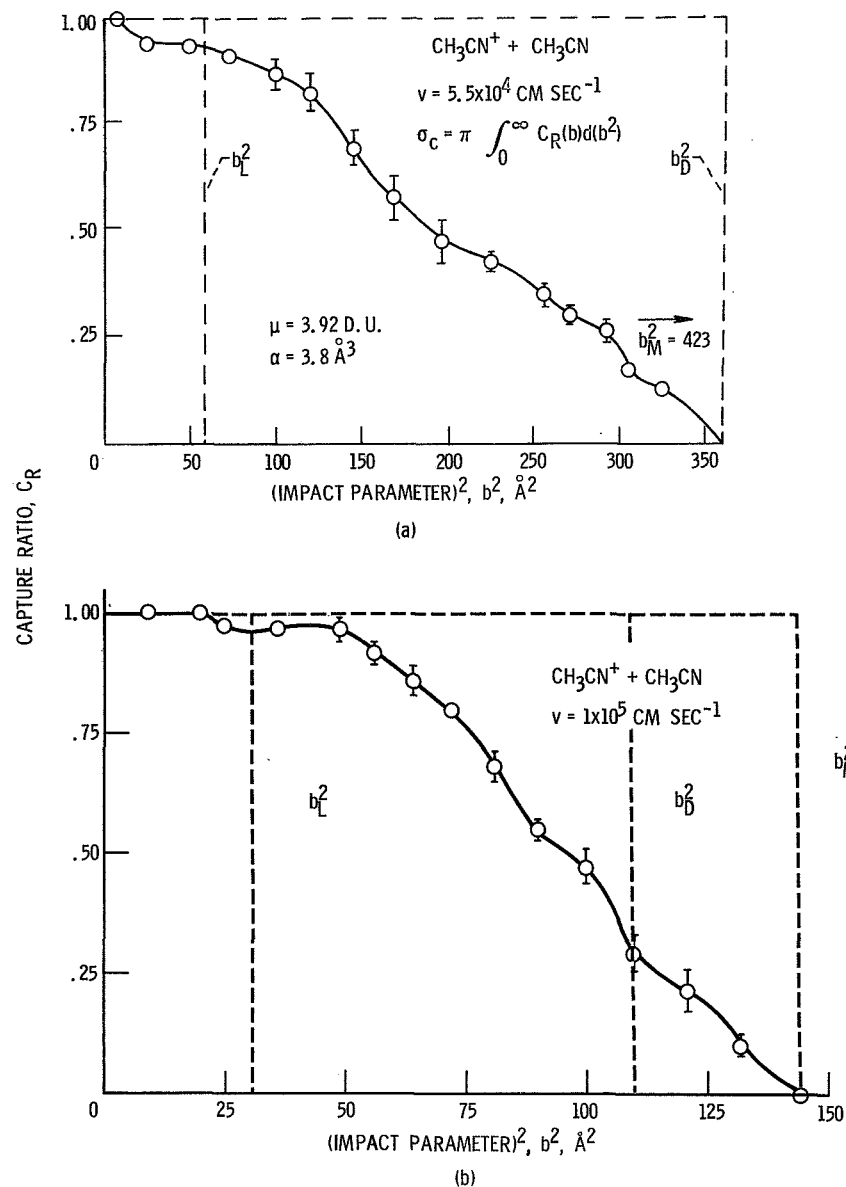


Figure 2. - Variation of capture ratio with square impact parameter for  $\text{CH}_3\text{CN}^+ + \text{CH}_3\text{CN}$  system. The symmetric top target rotators are distributed at temperature  $T_R = 500 \text{ K}$ . Bars indicate variation of calculation with different random number sets.

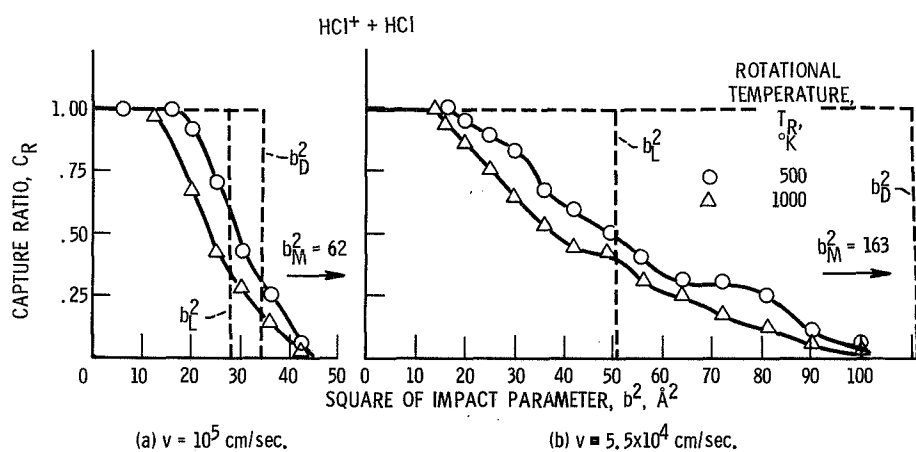
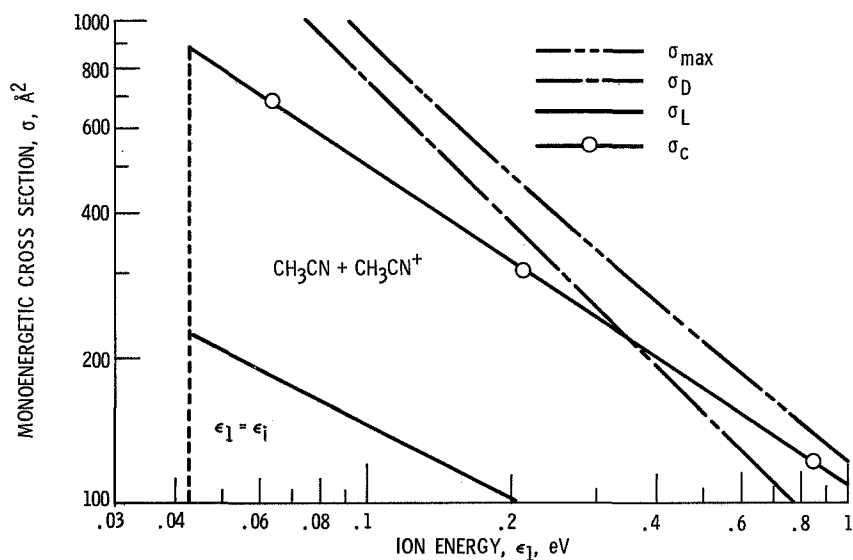
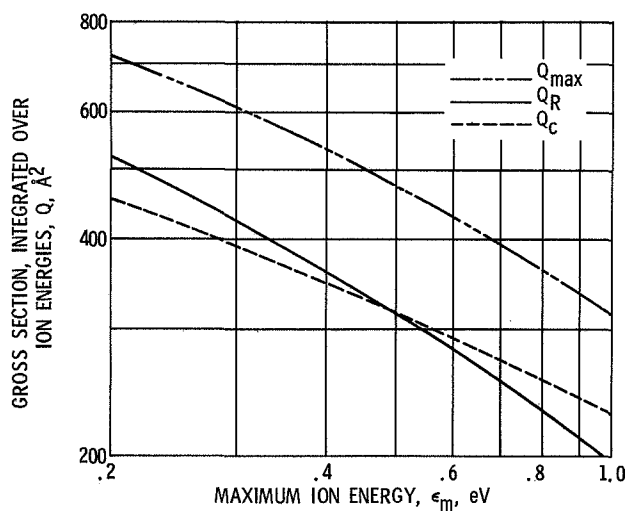


Figure 3. - Variation of capture ratio with square of impact parameter for linear HCl target rotators distributed at temperatures  $T_R = 500$  and  $1000$  K; 50 collisions were studied per point.

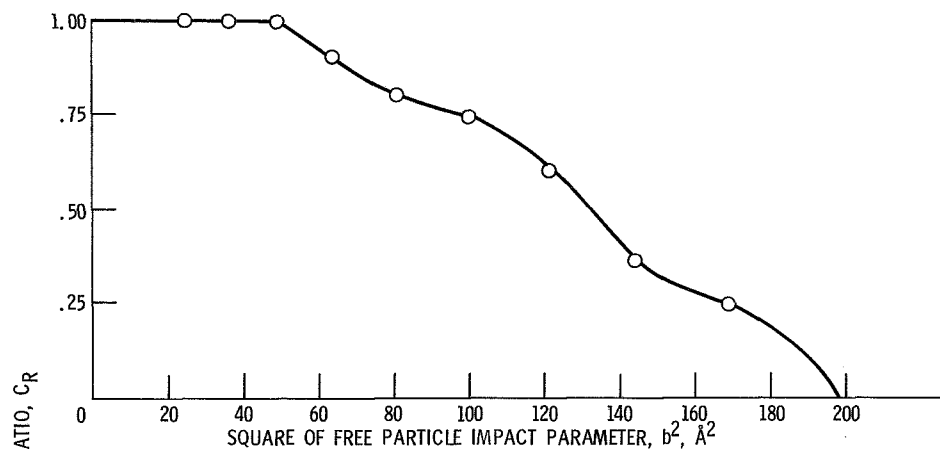


(a) Comparison of numerically calculated cross sections  $\sigma_c$  for methyl cyanide-parent ion collision with various theoretical cross sections. All cross sections are plotted as functions of ion translational energy for one rotational temperature  $T_R = 500$  K; electronic polarizability  $\alpha$ ,  $3.8 \text{ \AA}^3$ ; dipole moment  $\mu$ , 3.92 Debye units.

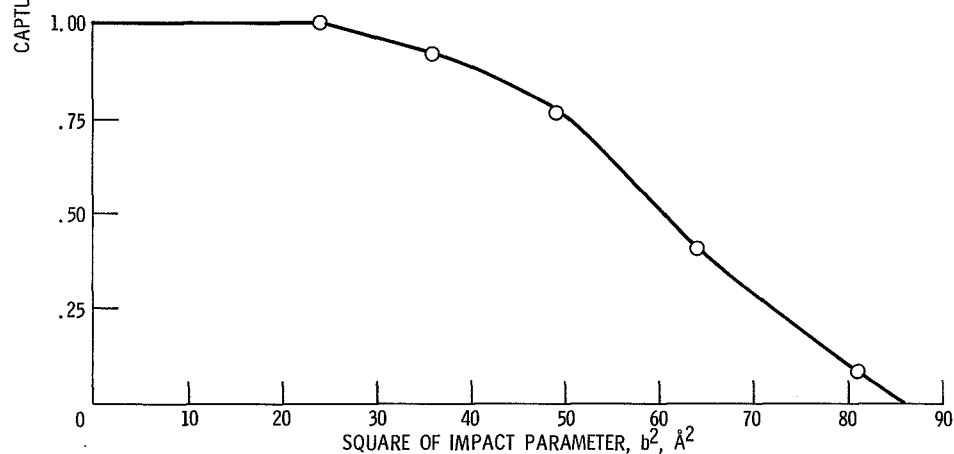


(b) Comparison of numerical capture cross section  $Q_c$  with experimentally assumed capture cross section  $Q_{\text{max}}$  and observed reaction cross section for methyl cyanide-parent ion collision as function of maximum ion energy  $\epsilon_m$ .

Figure 4

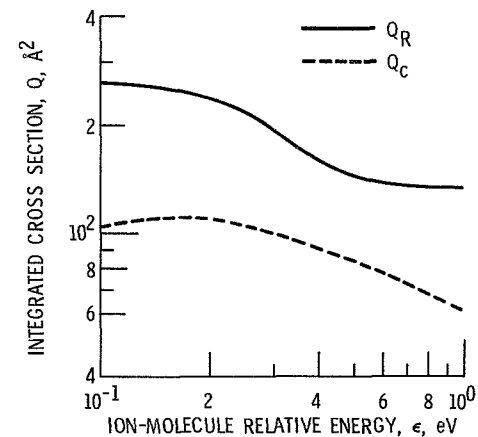


(a)  $\text{CH}_3\text{OH}^+ + \text{CH}_3\text{OH}$  capture;  $v = 5 \times 10^4 \text{ cm sec}^{-1}$ .



(b)  $\text{CH}_3\text{OH}^+ + \text{CH}_3\text{OH}$  capture;  $v = 10^5 \text{ cm sec}^{-1}$ .

Figure 5. - Variation of capture ratio with free-particle impact parameter for rotational temperature of 500 K. Methyl alcohol parent-ion collision.



(c) Comparison of integrated numerical capture cross section  $Q_C$  with experimentally observed capture cross section  $Q_R$  for methyl alcohol parent-ion collision.

Figure 5. - Concluded.

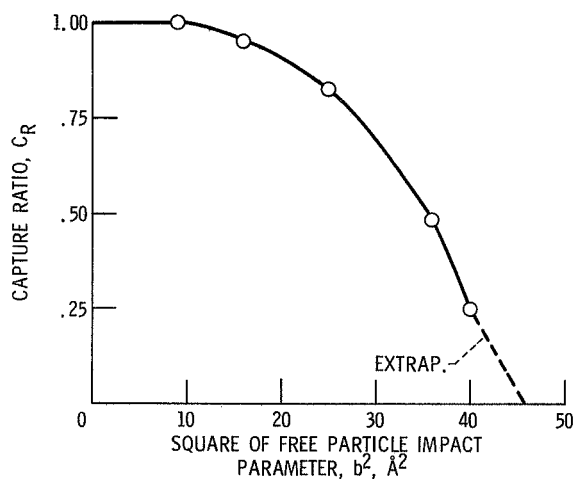


Figure 6. - Variation of capture ratio with free-particle impact parameter for rotational temperature of 500 K,  $\text{H}^- + \text{H}_2\text{O}$  capture collision;  $\epsilon = 0.2$  eV;  $v = 6.36 \times 10^5$  cm sec $^{-1}$ ; 50 transectories per point.

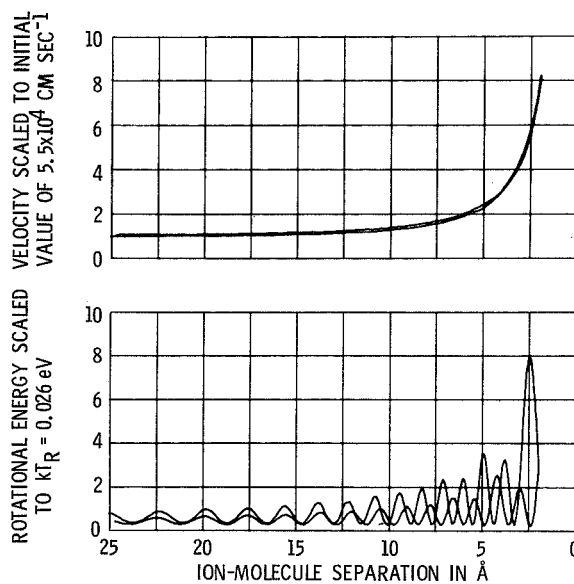


Figure 7. - Variation of ion velocity and polar molecule rotational energy during  $\text{NO}_2^+ + \text{HCl}$  single reflection capture collision.

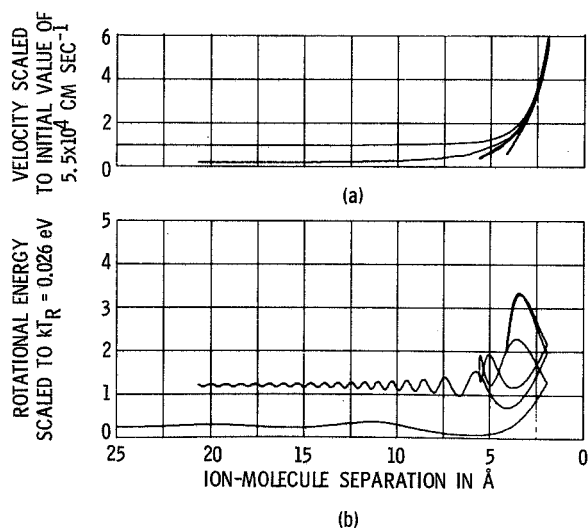


Figure 8. - Variation of ion velocity and polar molecule rotational energy during  $\text{Ar}^+ + \text{CO}$  multiple reflection capture collision.

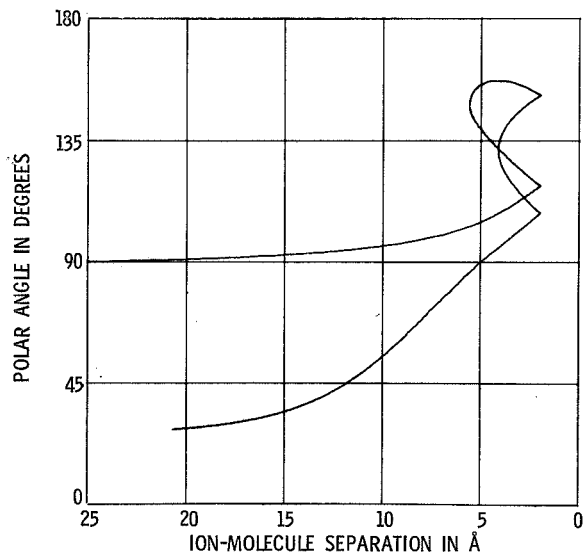


Figure 9. - Variations of polar angle  $\theta$  for translational motion of  $\text{Ar}^+$  relative to CO molecule during multiple reflection capture collision.



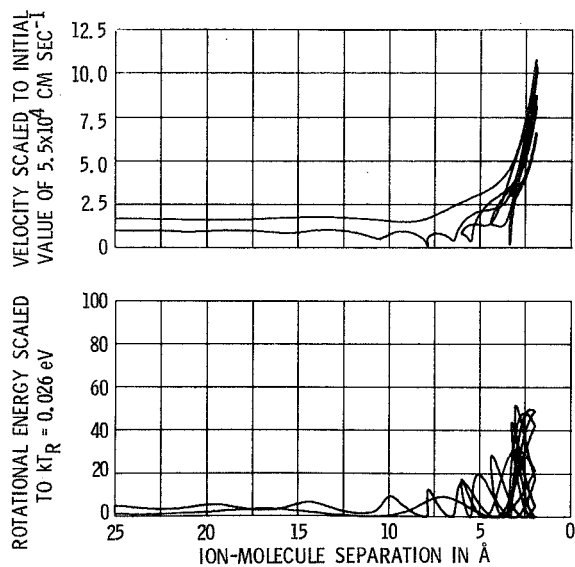


Figure 10. - Variation of ion velocity and polar molecule rotational energy during methyl cyanide-parent ion multiple reflection capture collision.

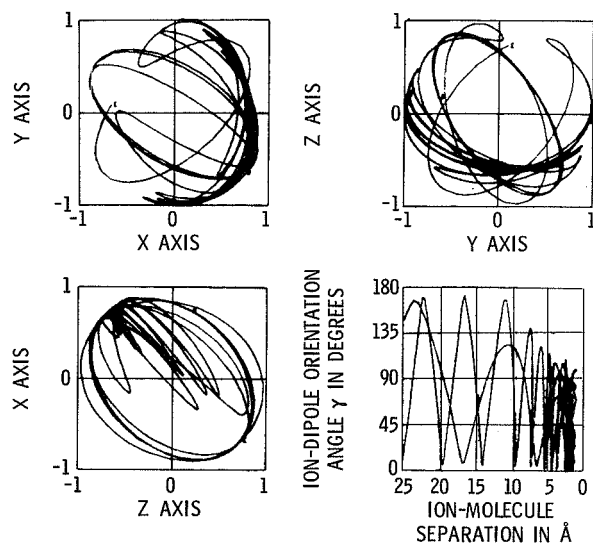


Figure 11. - Variations of dipole moment vector and ion-dipole orientation angle during  $\text{CH}_3\text{CN}-\text{CH}_3\text{CN}^+$  multiple reflection capture collision with several turning points.

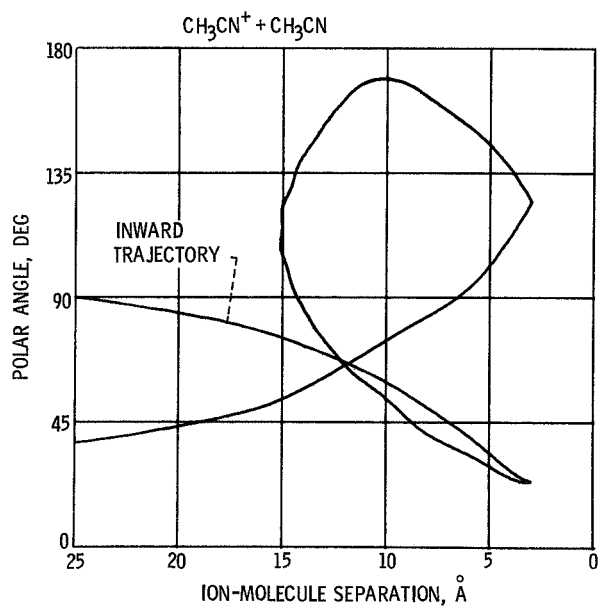


Figure 12. - Variation of polar angle for translational motion of  $\text{CH}_3\text{CN}^+$  relative to  $\text{CH}_3\text{CN}$  molecule during multiple reflection capture collision.

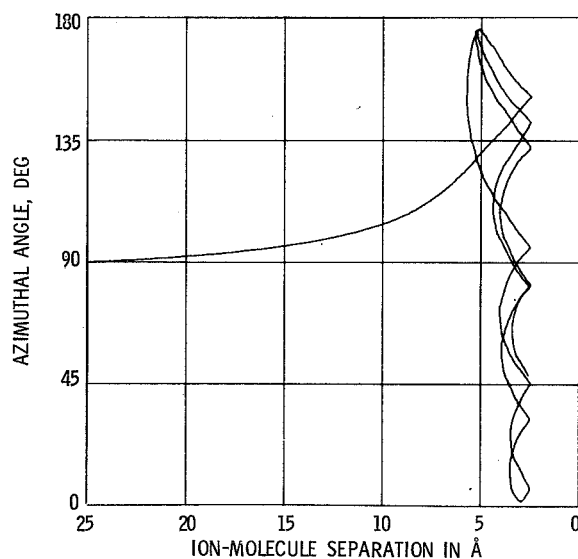


Figure 13. - Variations of azimuthal angle  $\phi$  for translational motion of  $\text{NO}_2^+$  relative to  $\text{HCl}$  molecule during multiple reflection capture collision.

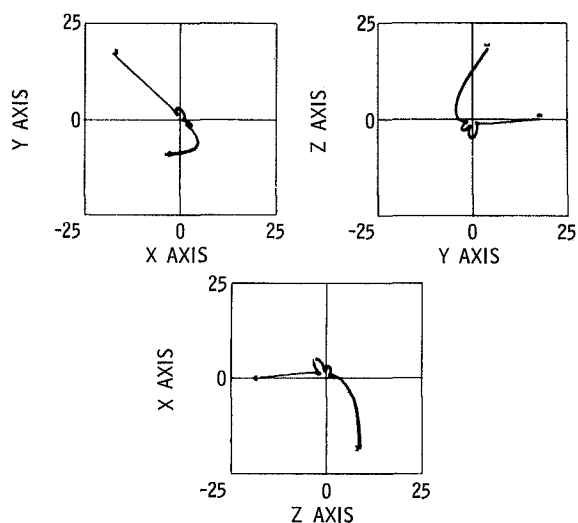


Figure 14. - Variation of ion projections tracing translational motion in  $\text{Ar}^+ + \text{CO}$  capture collision with multiple reflections.

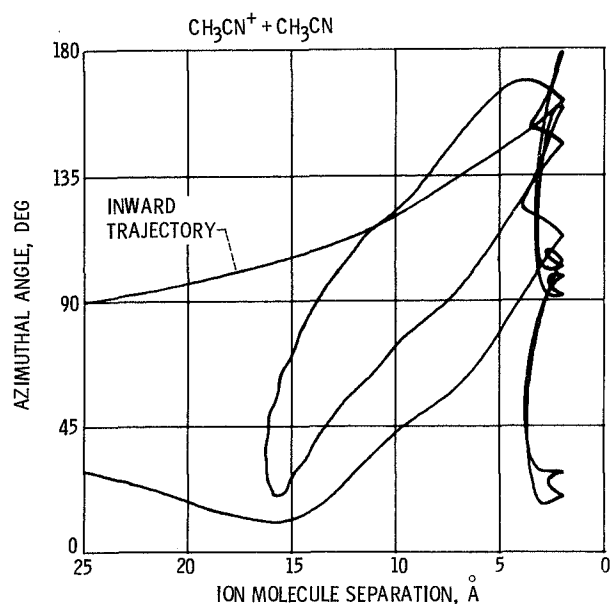


Figure 15. - Variation of azimuthal angle  $\varphi$  for translational motion of  $\text{CH}_3\text{CN}^+$  relative to  $\text{CH}_3\text{CN}$  molecule during multiple reflection capture collision with maximum turning point of 16 Å.

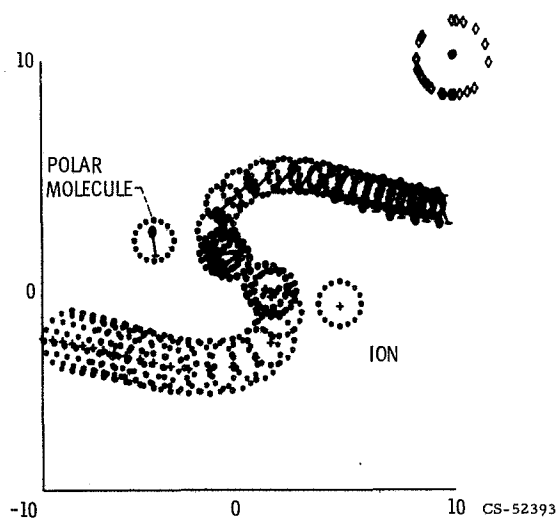


Figure 16. - Superposition of 15 movie frames for single reflection  $\text{CH}_3\text{CN}$  parent-ion collision. Ion-molecule pair are designated in pre-reflection positions; motion is traced during and after reflection.

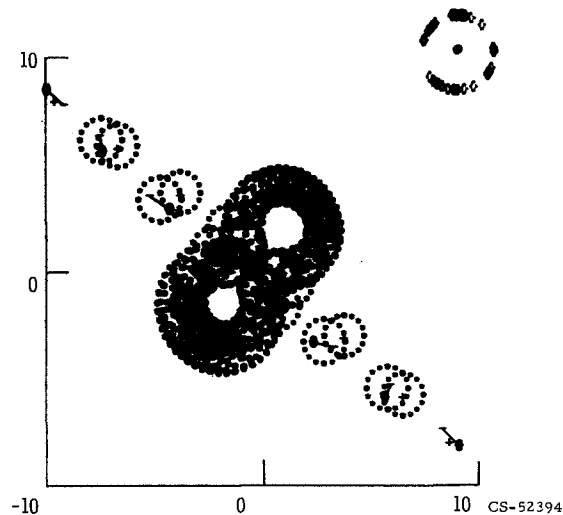


Figure 17. - Superposition of 40 movie frames demonstrating mutual spiraling of ion and molecule in  $\text{CH}_3\text{CN}$ -parent ion multiple reflection collision with zero degrees net scattering.